

Poissonian reducibility and thermal scaling within the lattice gas model and molecular dynamics model

Y. G. Ma

*China Center of Advanced Science and Technology (World Laboratory), P. O. Box 8730, Beijing 100080, CHINA
Shanghai Institute of Nuclear Research, the Chinese Academy of Sciences, P.O. Box 800-204, Shanghai 201800, CHINA
LPC, IN2P3-CNRS, ISMRA et Université, Boulevard Maréchal Juin, 14050 Caen Cedex, FRANCE*

The emission of cluster in the nuclear disassembly is investigated within the framework of isospin dependent lattice gas model and classical molecular dynamics model. As observed in the recent experimental data, it is found that the emission of individual cluster is poissonian and thermal scaling is observed in the linear Arrhenius plots made from the average multiplicity of each cluster. The mass, isotope and charge dependent "emission barriers" are extracted from the slopes of the Arrhenius plots and their possible physical implications are investigated.

PACS Number(s): 25.70.Pq, 05.70.Jk, 24.10.Pa, 02.70.Ns

In low-intermediate energy heavy ion collisions (HIC) the hot nuclei with moderate temperature can be formed and they finally deexcite by the different decay modes, such as the emission of multiple intermediate mass fragment (IMF), *i.e.* multifragmentation. Despite of the extensive studies in experiments and theories, it is still difficult to clarify whether the multifragmentation is statistical or dynamical, sequential or simultaneous. Recently Moretto et al. found that there exists the resilient reducibility and thermal scaling in multiple fragment emission process, which gives one a helpful and clear picture to look and understand the multifragmentation. They observed that the experimental Z -integrated fragment multiplicity distributions P_n^m are binomially distributed,

$$P_n^m(p) = \frac{m!}{n!(m-n)!} p^n (1-p)^{m-n} \quad (1)$$

in each transverse energy (E_t) window, where n is the number of emitted fragments and m is interpreted as the number of times the system tries to emit a fragment. The probability of emitting n fragments can be reduced to a single-particle emission probability p which gives linear Arrhenius plots (*i.e.* excitation functions) when $\ln(1/p)$ is plotted vs $1/\sqrt(E_t)$. By assuming a linear relationship between $\sqrt(E_t)$ and temperature T and from the linearity of the observed $\ln(1/p)$ vs $1/\sqrt(E_t)$ plot, it has been inferred that a thermal scaling of the multifragment process might be a general property [1-3]. In this case, these linear Arrhenius plots suggest that p has the Boltzmann form $p \propto \exp(-B/T)$ with a common fragment barrier B . However, since the binomial decomposition has been performed on the Z -integrated multiplicities, typically associated with $3 \leq Z \leq 20$, the Arrhenius plot generated with the resulting one fragment probability p is an average over a range of Z values. However, this kind of binomial reducibility and thermal scaling has been met with several debates [6-9]. Of which the one is that their assumption of a linear relationship between $\sqrt(E_t)$ and temperature T [6] in experimental

data. Tsang and Danielewicz pointed that the $T \propto \sqrt(E_t)$ assumption will break down for the intermediate energy HIC such as $^{36}\text{Ar} + ^{197}\text{Au}$ at $E/A = 35$ to 110 MeV due to the mid-rapidity particle production from the overlap region of projectile and target as well as the delayed emission from projectile-like and target-like residues. In this case the above interpretation of thermal scaling on emission probability is not valid in the point of experimental view. On the other side, the fit with the binomial distribution can be also replaced with the Poisson distribution in the constraint of charge conservation. In this context, the reducibility of fragment emission to binomial distributions does not imply any fundamental significance for the parameters m and p thereby extracted. If p is not an elementary emission probability, then the nuclear Arrhenius law will break down also.

Besides the binomial distribution for Z -integrated multiplicities, recently Beaulieu and Moretto et al. analyzed the behavior of individual fragment species of a given Z for higher resolution experimental data and noticed that the n -fragment multiplicities $P(n)$ obeyed a nearly Poisson distribution,

$$P(n) = \frac{\langle n \rangle^n e^{-\langle n \rangle}}{n!}, \quad (2)$$

where n is the number of fragments of a given Z and the average value $\langle n \rangle$ is a function of E_t , and were thus reducible to a single-fragment probability proportional to the average value $\langle n \rangle$ for each Z [4]. Similarly the $\langle n \rangle$ is found to be proportional to $\exp(-B/\sqrt(E_t))$, *i.e.* there exists also a thermal scaling law. As pointed out by Moretto et al. [5], this kind of "reducibility" and "thermal scaling" are empirically pervasive features of nuclear multifragmentation. "Reducibility" proves nearly stochastic emission process. "Thermal scaling" gives an indication of thermalization. In this work we would like to clarify that the Poissonian reducibility and thermal scaling is valid for fragment emission in nuclear multifragmentation via the theoretical reexamination of thermal equilibrium models.

In this Letter, we will analyze the fragment multiplicity distributions for each individual fragment Z and A value in the framework of isospin dependent lattice gas model (I-LGM) and classical molecular dynamics (I-CMD). We will show that they are Poissonian and the associated mean multiplicities for each Z or A give linear Arrhenius plots as the experimental data illustrated in [4]. The A and Z dependent barriers are extracted and investigated as a function of source size. Within our knowledge, this is the first time to explore the Poissonian reducibility and its thermal scaling for the individual fragment in the nuclear disassembly within the lattice gas model and molecular dynamics model.

The lattice gas model was developed to describe the liquid-gas phase transition for atomic system by Lee and Yang [10]. The same model has already been applied to nuclear physics for isospin symmetrical systems in the grand canonical ensemble [11] with a sampling of the canonical ensemble [12–18], and also for isospin asymmetrical nuclear matter in the mean field approximation [19]. In addition, a classical molecular dynamical model is used to compare with the results of lattice gas model. Here we will make a brief description for the models.

In the lattice gas model, A ($= N + Z$) nucleons with an occupation number s_i which is defined $s_i = 1$ (-1) for a proton (neutron) or $s_i = 0$ for a vacancy, are placed on the L sites of lattice. Nucleons in the nearest neighboring sites have interaction with an energy $\epsilon_{s_i s_j}$. The hamiltonian is written as

$$E = \sum_{i=1}^A \frac{P_i^2}{2m} - \sum_{i < j} \epsilon_{s_i s_j} s_i s_j, \quad (3)$$

where P_i is the momentum of the nucleon and m is its mass. The interaction constant $\epsilon_{s_i s_j}$ is chosen to be isospin dependent and be fixed to reproduce the binding energy of the nuclei [16]:

$$\begin{aligned} \epsilon_{nn} &= \epsilon_{pp} = 0 \text{ MeV}, \\ \epsilon_{pn} &= -5.33 \text{ MeV}. \end{aligned} \quad (4)$$

Three-dimension cubic lattice with L sites is used which results in $\rho_f = \frac{A}{L} \rho_0$ of an assumed freeze-out density of disassembling system, in which ρ_0 is the normal nuclear density. The disassembly of the system is to be calculated at ρ_f , beyond which nucleons are too far apart to interact. Nucleons are put into lattice by Monte Carlo Metropolis sampling. Once the nucleons have been placed we also ascribe to each of them a momentum by Monte Carlo samplings of Maxwell-Boltzmann distribution.

Once this is done the I-LGM immediately gives the cluster distribution using the rule that two nucleons are part of the same cluster if

$$P_r^2 / 2\mu - \epsilon_{s_i s_j} s_i s_j < 0, \quad (5)$$

where P_r is the relative momentum of two nucleons and μ is their reduced mass. This prescription is evidenced to be similar to the Coniglio-Klein's prescription

[20] in condensed matter physics and be valid in I-LGM [15,13,12,17]. To calculate clusters using I-CMD we propagate the particles from the initial configuration for a long time under the influence of the chosen force. The form of the force is chosen to be also isospin dependent in order to compare with the results of I-LGM. The potential for unlike nucleons is

$$\begin{aligned} v_{np}(r) \left(\frac{r}{r_0} < a \right) &= A \left[B \left(\frac{r_0}{r} \right)^p - \left(\frac{r_0}{r} \right)^q \right] \exp \left(\frac{1}{\frac{r}{r_0} - a} \right), \\ v_{np}(r) \left(\frac{r}{r_0} > a \right) &= 0. \end{aligned} \quad (6)$$

In the above, $r_0 = 1.842 \text{ fm}$ is the distance between the centers of two adjacent cubes. The parameters of the potentials are $p = 2$, $q = 1$, $a = 1.3$, $B = 0.924$, and $A = 1966 \text{ MeV}$. With these parameters the potential is minimum at r_0 with the value -5.33 MeV, is zero when the nucleons are more than $1.3r_0$ apart and becomes stronger repulsive when r is significantly less than r_0 . The potential for like nucleons is written as

$$\begin{aligned} v_{pp}(r) (r < r_0) &= v_{np}(r) - v_{np}(r_0), \\ v_{pp}(r) (r > r_0) &= 0. \end{aligned} \quad (7)$$

This means there is a repulsive core which goes to zero at r_0 and is zero afterwards. It is consistent with the fact that we do not put two like nucleons in the same cube. The system evolves for a long time from the initial configuration obtained by the lattice gas model under the influence of the above potential. At asymptotic times the clusters are easily recognized. The cluster distribution and the quantities based on it in the two models can now be compared. In the case of proton-proton interactions, the Coulomb interaction can also be added separately and compared with the cases where the Coulomb effects are ignored.

In this Letter we choose the medium size nuclei ^{129}Xe as a main example to analyze the behavior of individual fragment emission during nuclear disassembly with the helps of I-LGM and I-CMD. In addition, the systems with $A = 80$ and 274 are also studied to investigate the possible source size dependence. In this work, ρ_f is chosen to be about $0.38 \rho_0$, due to the experimental data can be best fitted by ρ_f between $0.3\rho_0$ and $0.4\rho_0$ in the previous LGM calculations [12,21], which corresponds to 7^3 cubic lattice is used for Xe, 6^3 for $A = 80$ and 9^3 for $A = 274$. In the condition of the fixed freeze-out density, the only input parameter of the models is the temperature T . In the I-LGM case, ρ_f can be thought as the freeze-out density but in the I-CMD case ρ_f is, strictly speaking, not a freeze-out density but merely defines the starting point for time evolution. However since classical evolution of a many particle system is entirely deterministic, the initialization does have in it all the information of the asymptotic cluster distribution, we will continue to call ρ_f as the freeze-out density. 1000 events are simulated for each T which ensures enough statistics.

One of the basic characters of the Poisson distribution Eq.(2) is the ratio $\sigma_{n_i}^2 / \langle n_i \rangle \rightarrow 1$ where $\sigma_{n_i}^2$ is the variance of the distribution and $\langle n_i \rangle$ is the mean multiplicity. The first step we will show is this ratio. We give these ratios for clusters classified with different masses (A), light charged isotopes (LCP) and atomic number (Z) for the disassembly of ^{129}Xe as a function of temperature in the framework of I-LGM and I-CMD with Coulomb in Figure 1. Obviously, the ratios are close to one except for protons, which indicates that they might belong to the Poisson distributions. This can be further supported by the multiplicity distribution in different temperature. For instance, Fig.2 show the quality of the Poisson fits to the charged particle multiplicity distribution for ^{129}Xe in the I-LGM case. These Poisson fits are excellent for all $Z \geq 2$ over the entire range of T . The same good Poisson fit is obtained in the cases of I-CMD. Thus we conclude that Poissonian reducibility is valid in the thermal-equilibrium lattice gas model or molecular dynamics.

To verify thermal scaling in the models, the dependence of the mean yield of clusters on temperature is considered. Consequently, we generate Arrhenius plots by plotting $\ln \langle n_Z \rangle$ vs $1/T$. Figure 3 give a family of these plots for the disassembly of ^{129}Xe within the framework of I-LGM (left panel) and I-CMD with Coulomb interaction (right panel). The observed Arrhenius plots are striking linear for the lower T side, and their slopes generally increase with increasing Z value. The contrary tendency reveals in the high T side where $\ln \langle n_Z \rangle$ increases with $1/T$, i.e. decreases with increasing T . In this case, nuclear Arrhenius plots of $\langle n \rangle$ with $1/T$ are not valid but the Poissonian reducibility still remains (see Fig. 2). This behavior of $\langle n \rangle$ at higher T is related to the branch of the fall of the multiplicity of IMF (N_{IMF}) with T where the disassembling system is in vaporization [23–25] and hence only the lightest clusters are dominated and the heavier clusters become fewer and fewer with increasing T . Afterwards we will focus on the branch of lower temperature to discuss the Arrhenius law. The overall linear trend illustrates that thermal scaling is also present when the individual fragments of a specific A , Z and LCP are considered.

From figure 3 the slope parameter can be directly extracted in the lower T side as a function of Z or A . In Ref. [4] Moretto et al. has interpreted these slope parameters as "emission barriers" of specific individual fragments. Figure 4 gives the emission barrier of individual fragments with different A , LCP and Z in the framework of I-LGM, I-CMD with/without Coulomb interaction. The error bar in the figure represents the error in the extraction of the slope parameter. The first indication from this figure is that the emission barrier in the I-LGM case is the nearly same as the I-CMD case without Coulomb force, which supports that I-LGM is equivalent to I-CMD without Coulomb interaction rather well when the nuclear potential parameter is moderately chosen, but I-LGM is a quick model to analyze the behavior of nuclear dissociations.

The inclusion of long-range Coulomb interaction makes the emission barrier of individual fragments much lower since the repulsion of Coulomb force reduces the attractive role of potential and hence make clusters escape easily. The second indication is that the emission barriers increase with A (Z) at low A (Z) values and tend to be saturated at high A (Z) ones. Similar experimental results have been observed in Ref. [4] for individual fragments with different Z . However, the middle panel of Fig. 4 shows that bare dependence of emission barrier of LCP on A in the fixed atomic number Z , which indicates that the Z dependence of barrier is perhaps more intrinsical, the A dependence is mostly due to the average effect over the species with the same A but different Z .

On the origin of these barrier, the surface energy and Coulomb energy would play the roles. If fragments are formed by coalescence into a relatively cold and dense nuclear drop out of a hot diluted source, a surface energy for the fragment would suggest barriers proportional to $Z^{2/3}(A^{2/3})$. In the case of I-LGM and I-CMD without Coulomb, we can try to fit the barrier for the particles with different mass number by

$$B_{Coul.off} = c_1 \times A_i^{2/3}, \quad (8)$$

or for the particles with different charge number by

$$B_{Coul.off} = c_1 \times ((A/Z)_{fit} * Z_i)^{2/3}, \quad (9)$$

where $(A/Z)_{fit}$ is a fit coefficient of A/Z for emitted particles, and A_i (Z_i) is the mass (charge) of particle. c_1 is the fit constant for surface energy term. The solid line in the Fig.4a is a function of Eq.(8) with $c_1 = 8.469$ and the solid line in the Fig.4c is a function of Eq.(9) with $c_1 = 8.469$ and $(A/Z)_{fit} = 1.866$. These excellent fits imply that the surface energy play a major role in controlling the cluster emission when the lone range Coulomb force is not considered. However for the cluster emission with the Coulomb field, we can assumed that the barrier is mainly constituted by the surface energy term and an additional Coulomb term as

$$B_{Coul.on} = c_2 \times A_i^{2/3} - \frac{1.44 \times A_i / (A/Z)_{fit} \times Z_{res}}{r_{Coul}(A_i^{1/3} + ((A/Z)_{fit} * Z_{res})^{1/3})} \quad (10)$$

for the particles with different mass number, or

$$B_{Coul.on} = c_2 \times ((A/Z)_{fit} * Z_i)^{2/3} - \frac{1.44 \times Z_i \times Z_{res}}{r_{Coul}((Z_i / (A/Z)_{fit})^{1/3} + (Z_{res} / (A/Z)_{fit})^{1/3})} \quad (11)$$

for the particles with different charge number, where c_2 is a fit constant for surface term and r_{Coul} is chosen to be 1.22 fm. Z_{res} is a fitted average charge number of the residue. $(A/Z)_{fit}$ is chosen to be 1.866, as taken from the fits for I-LGM. The overall fits for A and Z

dependent barrier in the case of I-CMD with Coulomb force give $c_2 = 12.921$ and $Z_{res} \sim 41$ with the dot-dashed line in Fig.4a and 4c. The excellent fit supports that the Coulomb energy plays another important role in the cluster emission.

In the case of I-LGM and I-CMD without Coulomb, one would expect the barrier for each Z (A) to be nearly independent of the system studied if only the surface energy is substantial to the emission barrier. The left panel of the figure 5 shows the results for B_A , B_{LCP} and B_Z for three different systems in the I-LGM case. The same freeze-out density of $0.38\rho_0$ and the same N/Z is chosen for the systems of $A=80$ and $A = 274$. Actually, it appears to have no obvious dependence of emission barrier on source size as expected for the role of surface energy. The solid line in the figure is the same as in Fig.4. However, when the long-range Coulomb interaction is considered, the emission barrier reveals a source size dependence. The right panel of figure 5 gives the emission barriers B_A , B_{LCP} and B_Z in the case of I-CMD with Coulomb force. It looks that the barrier increase with the decreasing of charge of system, which can be explained with the Eq. (10) and (11) where the decreasing of the residue Z_{res} will result in the decreasing of the Coulomb barrier and hence the increasing of the emission barrier. The lines represent the fits with the Eq.(10) and (11) for three different mass systems.

In conclusion, the poisson reducibility and thermal scaling of the emitted cluster is explored in the lattice gas model and molecular dynamical model. The calculations are qualitatively consistent with the recent experimental observation by Morretto/Wozniak's group even though the temperature is supposed to be proportional to total transverse energy in the latter experiments. A systematic study of the emission barrier on the cluster mass, isotope and charge proves that the cluster emission is mainly controlled by both the surface energy and the Coulomb interaction. In the framework of the lattice gas model and molecular dynamics model without the Coulomb interaction, the emission barrier relies on the cluster charge with the $Z^{2/3}$ ($A^{2/3}$) law and it does not depend on the the source size, which indicates that the surface energy play a basic dominant role to control the cluster emission. Conversely, in the framework of molecular dynamics model with the Coulomb force, the emission barrier will decrease strongly according to the Eq.(10) and (11) and it decreases with the increasing of the source size, illustrating that the Coulomb interaction play another important role to control the cluster emission.

ACKNOWLEDGMENTS

Author would like to thank Prof. B. Tamain, Prof. S. Das Gupta, Prof W.Q. Shen and Dr. J.C. Pan for helps. This work was supported in part by the NSFC for

Distinguished Young Scholar under Grant No. 19725521, the NSFC under Grant No. 19705012, the Special Foundation of the President of Chinese Academy of Sciences, the Major State Basic Research Development Program of China under Contract No. G200077400. It was also supported partly by the IN2P3-CNRS Foundation of France.

- [1] L.G. Moretto et al., Phys. Rev. Lett. **74**, 1530 (1995).
- [2] K. Tso et al., Phys. Lett. B **361**, 25 (1995).
- [3] L. G. Moretto, R. Gettim L. Phair, K. Tso. and G.J. Wozniak, Phys. Rep. **79**, 249 (1997).
- [4] L. Beaulieu, L. Phair, L.G. Moretto and G.J. Wozniak, Phys. Rev. Lett. **81**, 770 (1998).
- [5] L.G. Moretto, L. Phair, and G.J. Wozniak, Phys. Rev. C **60**, (1999).
- [6] M.B. Tsang and P. Danielewicz, Phys. Rev. Lett. **80**, 1178 (1998).
- [7] A. Wieloch et al., Z. Phys. A **359**, 345 (1997); Phys. Lett. B **432**, 29 (1998).
- [8] J. Toke et al., Phys. Rev. C **56**, R1683 (1997).
- [9] A.S. Botvina and D.H. Gross, Phys. Rev. C **58**, R23 (1998).
- [10] T.D. Lee and C.N. Yang, Phys. Rev. **87**, 410 (1952).
- [11] T.S. Biro et al., Nucl. Phys. A **459**, 692 (1986); S.K. Samaddar and J. Richert, Phys. Lett. B **218**, 381 (1989); Z. Phys. A **332**, 443 (1989); J.M. Carmona et al., Nucl. Phys. A **643**, 115 (1998).
- [12] J. Pan and S. Das Gupta, Phys. Lett. B **344**, 29 (1995); Phys. Rev. C **51**, 1384 (1995); Phys. Rev. Lett. **80**, 1182 (1998); S. Das Gupta et al., Nucl. Phys. A **621**, 897 (1997).
- [13] J. Pan and S. Das Gupta, Phys. Rev. C **53**, 1319 (1996).
- [14] W.F.J. Müller, Phys. Rev. C **56**, 2873 (1997).
- [15] X. Campi and H. Krivine, Nucl. Phys. A **620**, 46 (1997).
- [16] J. Pan and S. Das Gupta, Phys. Rev. C **57**, 1839 (1998).
- [17] Ph. Chomaz and F. Gulminelli, Phys. Lett. B **447**, 221 (1999).
- [18] Y.G. Ma, Phys. Rev. Lett. **83**, 3617 (1999); Phys. Rev. C **60**, 024607 (1999).
- [19] S. Ray et al., Phys. Lett. B **392**, 7 (1997).
- [20] A. Coniglio and E. Klein, J. Phys. A **13**, 2775 (1980).
- [21] L. Beaulieu et al., Phys. Rev. C **54**, R973 (1996).
- [22] L.G. Moretto et al., Phys. Rev. Lett. **71**, 3935 (1993).
- [23] C.A. Ogilvie et al., Phys. Rev. Lett. **67**, 1214 (1991).
- [24] M.B. Tsang et al., Phys. Rev. Lett. **71**, 1502 (1993).
- [25] Y.G. Ma and W.Q. Shen, Phys. Rev. C **51**, 710 (1995).

Fig.1: The ratio of $\sigma_i^2 / \langle n_i \rangle$ for the clusters classified with mass, light isotope mass and atomic number as a function of temperature. The left panel is for the I-LGM calculation and the right for I-CMD with Coulomb. The symbols are illustrated on the figure.

Fig.2: The excitation functions P_n for elements with $Z \geq 2$ emission from the source ^{129}Xe in the I-LGM calculation. The lines are Poisson fits with Eq.(2).

Fig.3: The average yield per event of different clusters classified with A (top), LCP (middle) and Z (bottom) as a function of $1/T$. The left panel is for the I-LGM calculation and the right for I-CMD with Coulomb. The solid lines are fits to the calculations using a Boltzmann factor for $\langle n_i \rangle$. The symbols are illustrated on the figure.

Fig.4: The emission barrier extracted from the Arrhenius plots as a function of cluster mass (top), isotopic mass (middle) or cluster charge (bottom) in the cases of I-LGM (solid squares), I-CMD without Coulomb (solid circles) and with Coulomb (open circles). The solid lines are fits with the Eq. (8) or (9), and the dot-dashed lines represent the fits with the Eq. (10) or (11).

Fig.5: The source size dependence of the emission barrier for the clusters classified with mass (top), isotopic mass (middle) or cluster charge (bottom) in the cases of I-LGM (left panel), I-CMD with Coulomb (right panel). The lines in the left panel are fits with the Eq. (8) or (9), and the solid, dot-dashed and dotted line in the right panel represents the fits to the emission barrier of $A = 80, 129$ and 274 , respectively, with the Eq. (10) or (11).

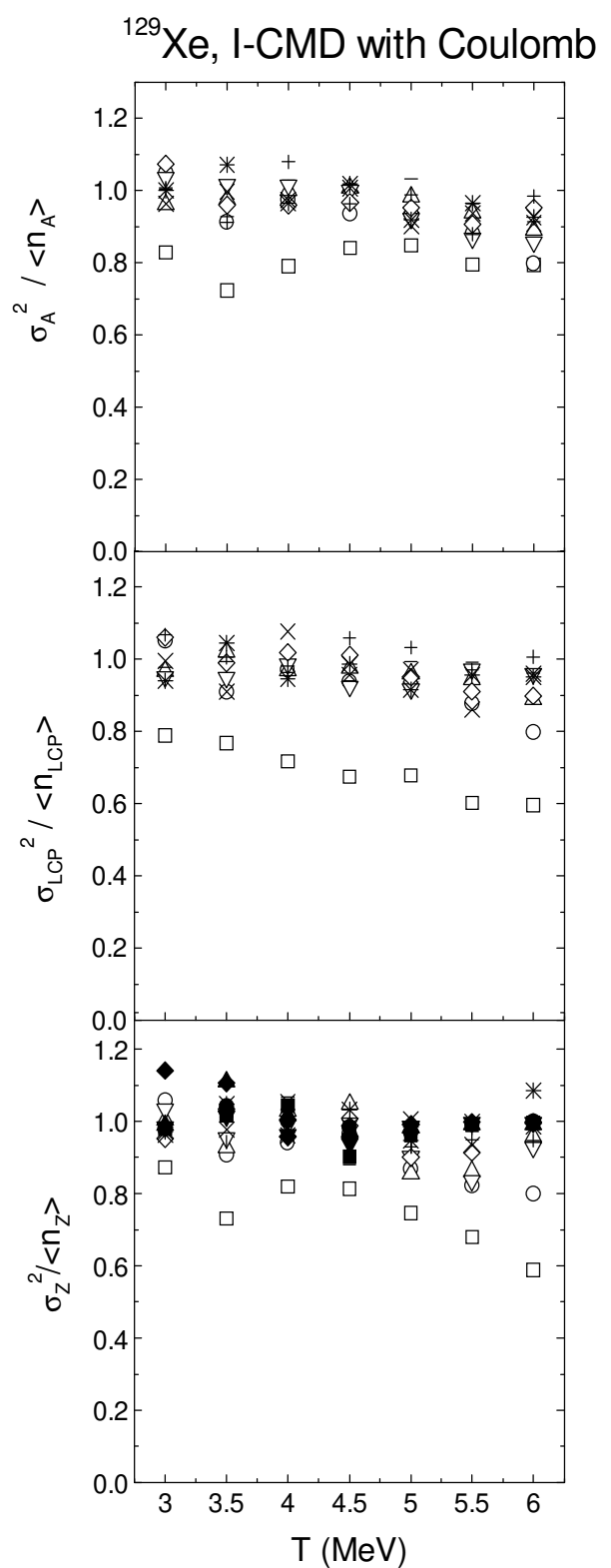
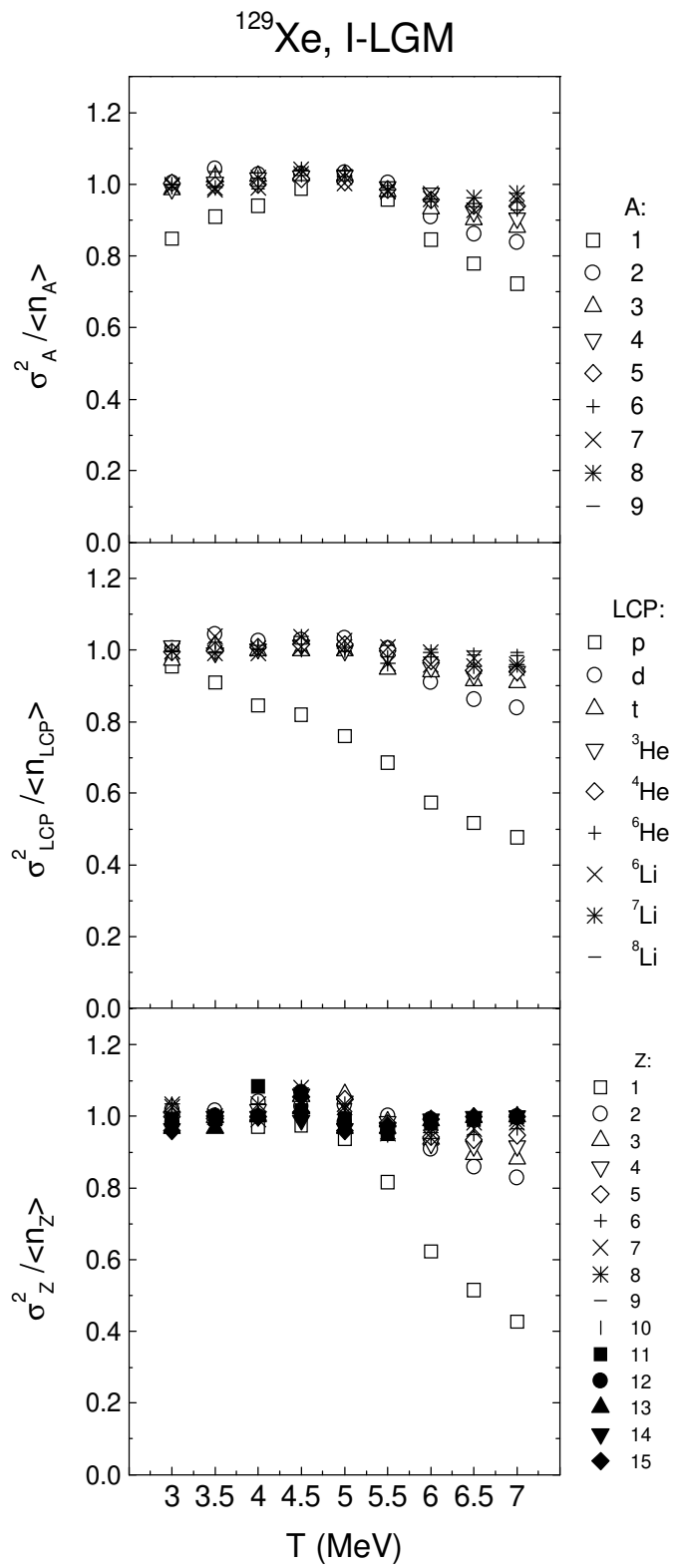


Fig. 1

^{129}Xe , I-LGM

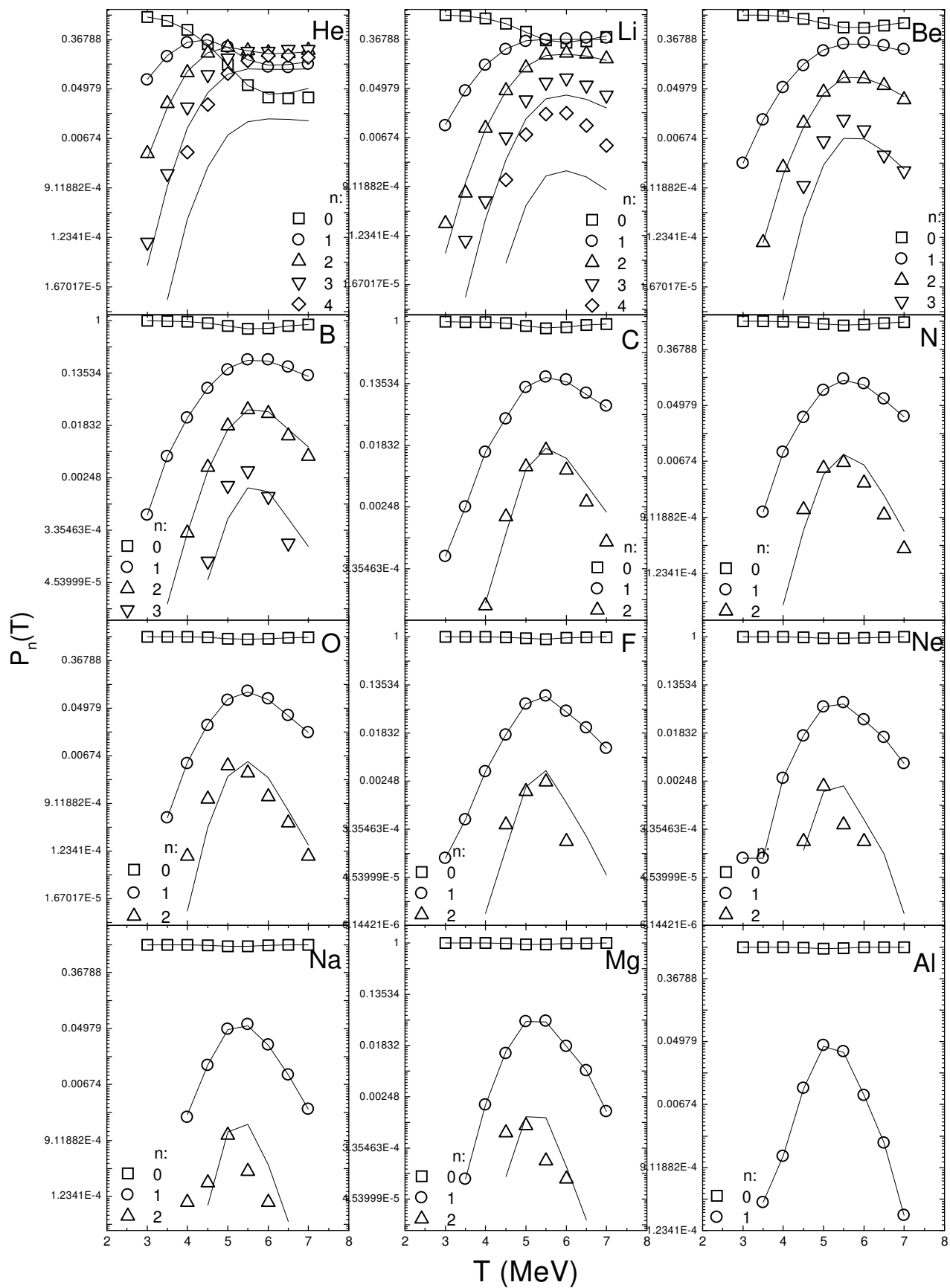
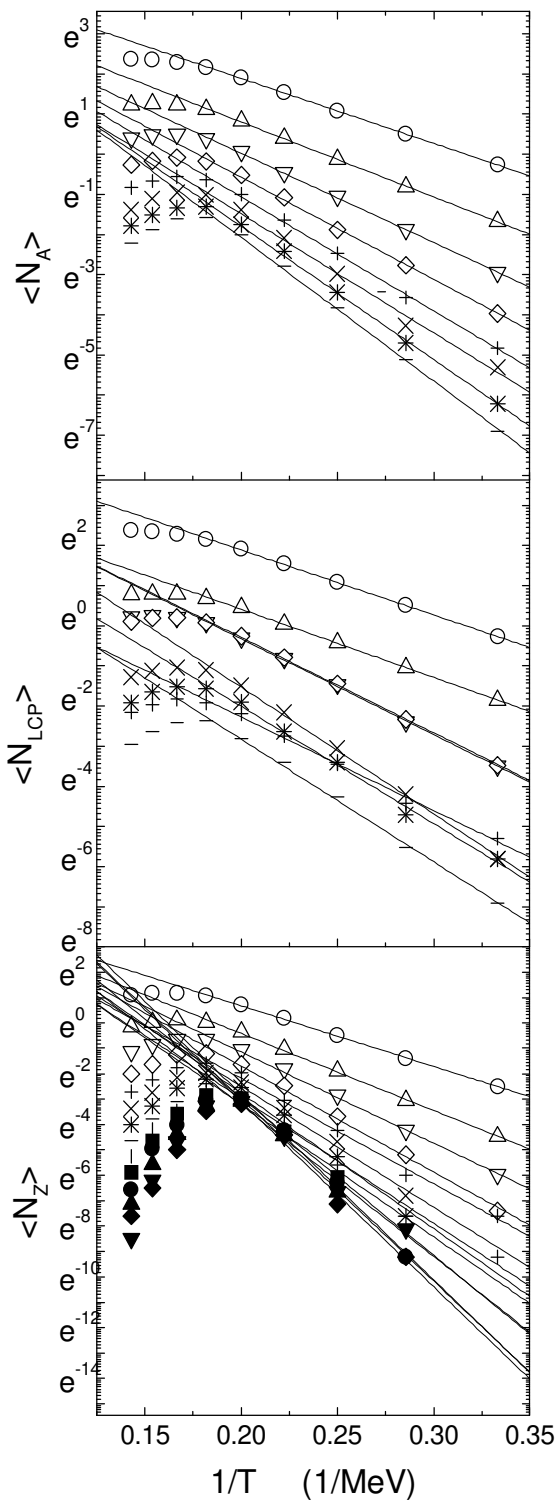


Fig. 2

^{129}Xe , I-LGM



^{129}Xe , I-CMD with Coulomb

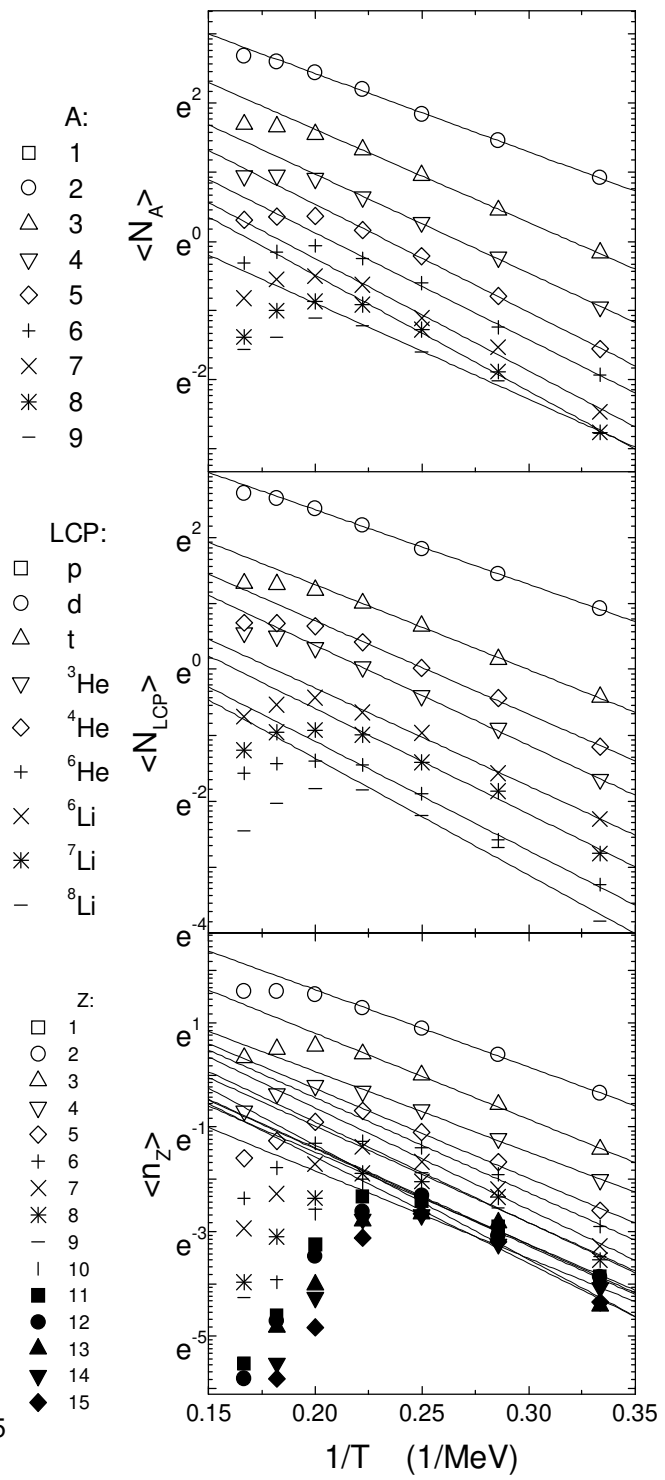


Fig. 3

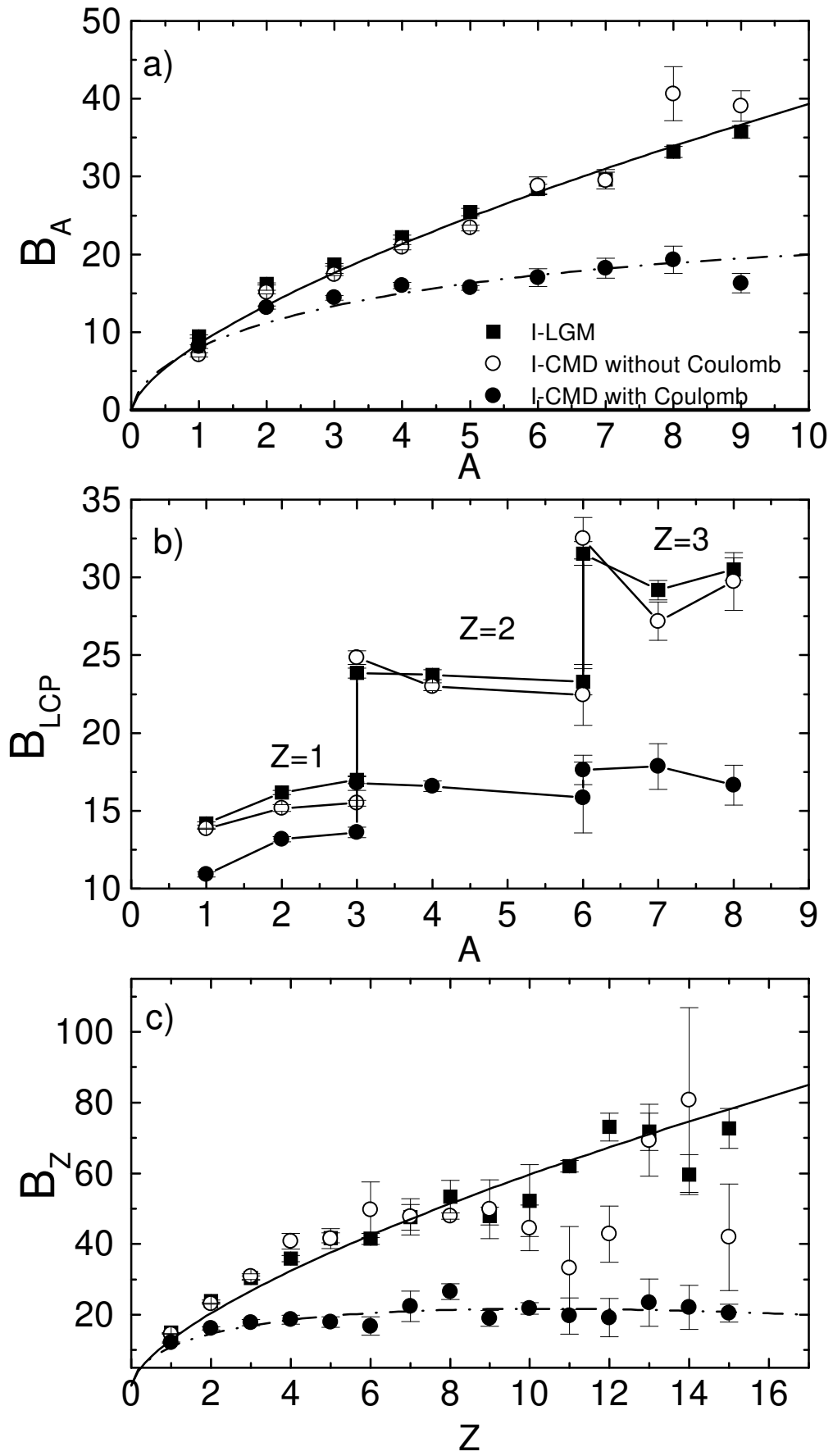


Fig. 4

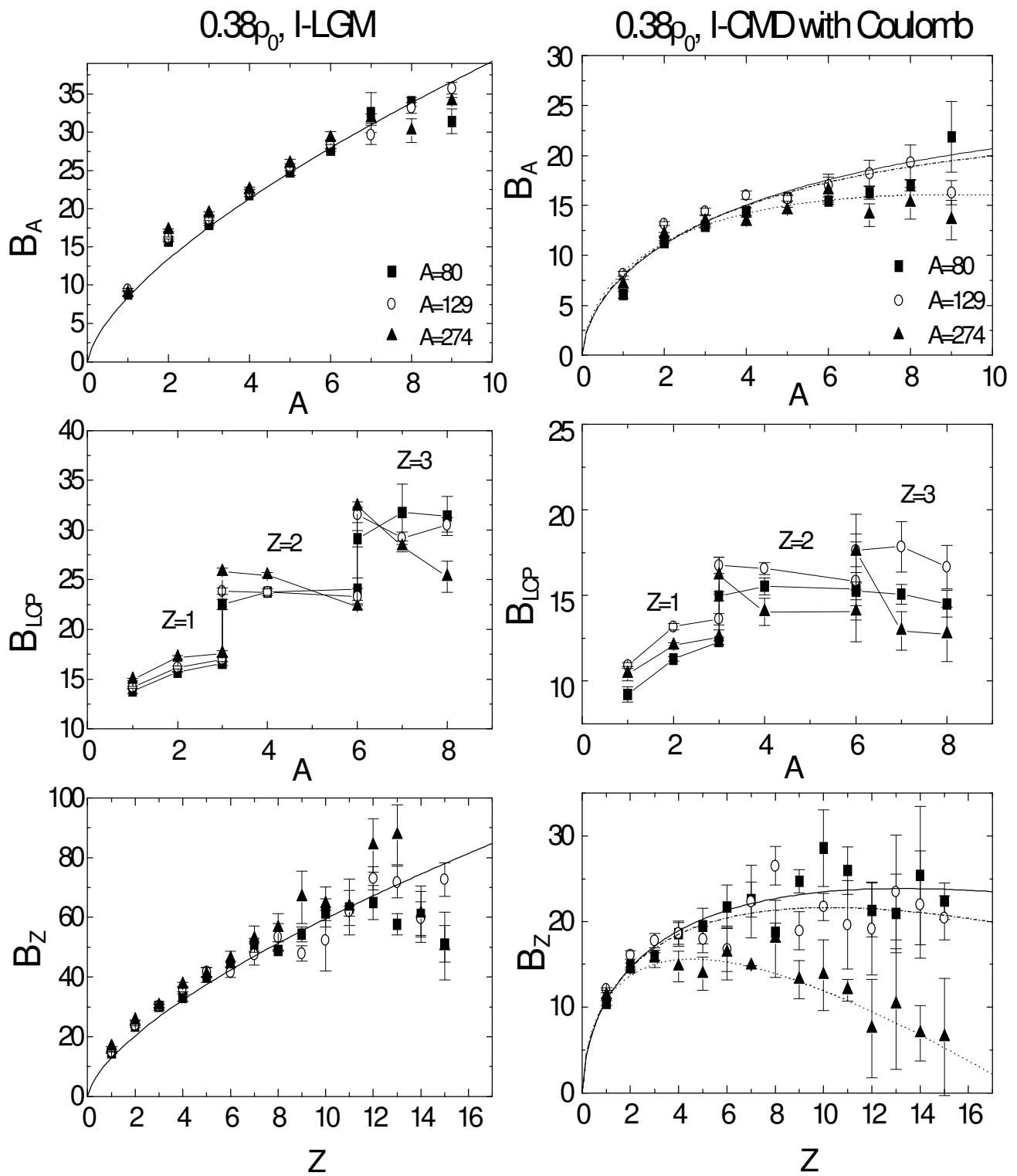


Fig. 5

